Blood Cells, Molecules and Diseases 79 (2019) 102346

Contents lists available at ScienceDirect

Blood Cells, Molecules and Diseases

journal homepage: www.elsevier.com/locate/bcmd

Combined genetic disruption of K-Cl cotransporters and Gardos channel KCNN4 rescues erythrocyte dehydration in the SAD mouse model of sickle cell disease

Boris E. Shmukler[a,b,1], Alicia Rivera[a,c,d,1], Parul Bhargava[e], Katherine Nishimura[a], Ann Hsu[a], Edward H. Kim[a], Marie Trudel[f], Marco B. Rust[g], Christian A. Hubner[h], Carlo Brugnara[b,d], Seth L. Alper[a,c,*]

[a] Renal Division and Vascular Biology Research Center, Beth Israel Deaconess Medical Center, Boston, MA, United States of America
[b] Department of Laboratory Medicine, Boston Children's Hospital, Boston, MA 02115, United States of America
[c] Department of Medicine, Harvard Medical School, Boston, MA 02115, United States of America
[d] Department of Pathology, Harvard Medical School, Boston, MA 02115, United States of America
[e] Department of Laboratory Medicine, UCSF, San Francisco, CA, United States of America
[f] Institut de Recherches Cliniques de Montreal, Molecular Genetics and Development, Faculte de Medecine, Universite of Montreal, Montreal, Quebec, Canada
[g] Institute of Physiological Chemistry, Philipps-Universität Marburg, Marburg, Germany
[h] Institute of Human Genetics, Universitatsklinikum Jena, Jena, Germany

ARTICLE INFO

Editor: Mohandas Narla

Keywords:
Red blood cell
Potassium transporter
Potassium channel
Osmotic fragility
Splenomegaly

ABSTRACT

Excessive red cell dehydration contributes to the pathophysiology of sickle cell disease (SCD). The densest fraction of sickle red cells (with the highest corpuscular hemoglobin concentration) undergoes the most rapid polymerization of deoxy-hemoglobin S, leading to accelerated cell sickling and increased susceptibility to endothelial activation, red cell adhesion, and vaso-occlusion. Increasing red cell volume in order to decrease red cell density can thus serve as an adjunct therapeutic goal in SCD. Regulation of circulating mouse red cell volume and density is mediated largely by the Gardos channel, KCNN4, and the K-Cl cotransporters, KCC3 and KCC1. Whereas inhibition of the Gardos channel in subjects with sickle cell disease increased red cell volume, decreased red cell density, and improved other hematological indices in subjects with SCD, specific KCC inhibitors have not been available for testing. We therefore investigated the effect of genetic inactivation of KCC3 and KCC1 in the SAD mouse model of sickle red cell dehydration, finding decreased red cell density and improved hematological indices. We describe here generation of mice genetically deficient in the three major red cell volume regulatory gene products, KCNN4, KCC3, and KCC1 in C57BL6 non-sickle and SAD sickle backgrounds. We show that combined loss-of-function of all three gene products in SAD mice leads to incrementally increased MCV, decreased CHCM and % hyperchromic cells, decreased red cell density (phthalate method), increased resistance to hypo-osmotic lysis, and increased cell K content. The data show that combined genetic deletion of the Gardos channel and K-Cl cotransporters in a mouse SCD model decreases red cell density and improves several hematological parameters, supporting the strategy of combined pharmacological inhibition of these ion transport pathways in the adjunct treatment of human SCD.

1. Introduction

Sickle cell disease affects approximately 80–100,000 individuals in the US, mostly of African descent, and many millions overseas. The disease is uniformly caused by the Glu-Val substitution at amino acid 6 of the hemoglobin beta chain, encoding sickle β-globin [25], but its clinical manifestations reflect the actions of numerous modifier genes. Although *ex vivo* gene replacement therapy with competitive transplant of genetically corrected hematopoietic stem cells can be curative [15], this promising approach is unlikely to be applicable to most patients in the near future.

Treatments to induce HbF also hold great promise. The effectiveness

* Corresponding author at: Renal Division, Beth Israel Deaconess Medical Center, 99 Brookline Ave. RN380F, Boston, MA 02215, United States of America.
E-mail address: salper@bidmc.harvard.edu (S.L. Alper).
[1] Equal contributions of Drs. Shmukler and Rivera as co-first authors.

https://doi.org/10.1016/j.bcmd.2019.102346
Received 14 May 2019; Received in revised form 9 July 2019; Accepted 9 July 2019
Available online 17 July 2019
1079-9796/

of hydroxyurea is due in large part to its induction of HbF, but up to 40% of sickle disease patients do not respond to the drug [26]. Butyrate derivatives and other more specific chromatin and DNA methylation modifiers have shown impressive efficacy but have been limited by later onset loss-of-efficacy or toxicity. Recently, inhibition of BCL11 expression has shown great promise as the strongest inducer of HbF to date [4]. However, additional adjunct pharmacological approaches are likely to remain necessary for the range of clinical presentations [22].

One such alternate approach is the therapeutic reduction of intracellular HbS concentration by modulation of sickle red cell potassium content and cell volume. Among the major regulators of sickle red cell potassium content are the SLC12 KCC potassium chloride transporters and the intermediate conductance calcium-activated potassium channel, KCNN4, also known as the Gardos channel. Nanomolar potency inhibitors of the Gardos channel, such as clotrimazole, TRAM-34, and senicapoc, have been shown to increase red cell K content and decrease mean corpuscular hemoglobin concentration in mouse models of sickle cell disease [8,21]. Senicapoc has been shown to have the same benefits in phase II and III clinical trials in humans with sickle cell disease [1,2]. These studies have confirmed the utility of KCNN4 as a therapeutic target in sickle cell disease. However, the KCC K-Cl cotransporters lack inhibitors of high affinity and high specificity, and are not at the stage of clinical investigation.

The SAD transgenic mouse model of human SCD was the first such mouse model [24]. Although superseded for most studies by subsequently developed human globin gene knock-in mouse models of human SCD, the SAD mouse remains valuable in modeling human sickle red cell dehydration more faithfully than other mouse models [8,12,18]. SAD mice also offer a simpler genetic structure than the more recent multi-locus genetically modified mouse models of sickle disease, facilitating their further genetic modification.

Therefore, we created in the transgenic SAD sickle hemoglobin background mouse models of sickle disease lacking the major erythroid KCC transporters, KCC3 and KCC1, lacking KCNN4, or with combined genetic deficiency of KCC3, KCC1, and KCNN4, to assess the abilities of these transporters to regulate sickle red cell volume and hydration status in a mouse model. Our results demonstrate the potential therapeutic utility of combined inhibition of KCNN4 and KCC3 in SAD mouse sickle RBC, and support continued investigation of sickle red cell volume regulation as an adjunct therapy for human sickle cell disease.

2. Materials and methods

2.1. Materials

All salts were from Sigma-Aldrich (St. Louis, MO) and were of reagent grade. Staurosporine was from Calbiochem (San Diego, CA). All other drugs were from Sigma-Aldrich or Aldrich.

2.2. Mice

Mice were housed in humidity- and temperature-controlled rooms in the Animal Research Facility of Beth Israel Deaconess Medical Center, with free access to water and food. SAD transgenic mice [8,18,24], exon 1-deleted *Kcnn4*$^{-/-}$ mice [3], K-Cl cotransporter-deficient mice (*Kcc1*$^{-/-}$;*Kcc3*$^{-/-}$ double knockout mice), and SAD;*Kcc1*$^{-/-}$;*Kcc3*$^{-/-}$ (SAD double knockout or SAD;2xKO) mice [18] were generated and genotyped as previously described. SAD;*Kcnn4*$^{-/-}$ mice were created by crossing SAD mice with *Kcnn4*$^{-/-}$ mice, and were born and weaned in numbers equivalent to those of *Kcnn4*$^{-/-}$ and WT^{Kcnn4} mice. *Kcc1*$^{-/-}$;*Kcc3*$^{+/-}$ mice were crossed with *Kcnn4*$^{-/-}$, and progeny of these matings were further intercrossed to generate *Kcc1*$^{-/-}$;*Kcc3*$^{-/-}$;*Kcnn4*$^{-/-}$ (3xKO) mice. SAD;*Kcnn4*$^{-/-}$ mice were crossed with *Kcc1*$^{-/-}$;*Kcc3*$^{+/-}$ mice to generate SAD;*Kcc1*$^{-/-}$;*Kcc3*$^{-/-}$;*Kcnn4*$^{-/-}$ (SAD;3xKO) mice. Wild type mice used for comparison with knockout mice were wild type progeny of SAD × WT C57BL6/J crosses (WT^{SAD}) and JAX C57BL6/J mice (WT^{C57}). Wild type mice used for comparison with Kcnn4$^{-/-}$ mice were wild type (*Kcnn4*$^{+/+}$) progeny of *Kcnn4*$^{-/+}$ breeding pairs (WT^{Kcnn4}).

Nearly all K-Cl cotransport activity of mouse red cells is mediated by KCC3 [18]. However, *Kcc3*$^{-/-}$ weanlings constituted only 50% of predicted numbers, and among these only 63% of weanlings survived to 6 weeks of age. In contrast, *Kcc1*$^{-/-}$;*Kcc3*$^{-/-}$ weanlings constituted 75% of predicted numbers, and 100% of these weanlings survived beyond 6 weeks of age, whereas births of SAD;*Kcc1*$^{-/-}$;*Kcc3*$^{-/-}$ mice were few, and survival poor. 3xKO and SAD;*Kcnn4*$^{-/-}$;*Kcc1*$^{-/-}$;*Kcc3*$^{-/-}$ (SAD;3xKO) weanlings also exhibited 93–100% survival to age 6 weeks and beyond. The mechanism by which lack of KCC1 expression enhanced survival of mice deficient in KCC3 alone or in combination with KCNN4 remains unclear.

2.3. Histology

Spleen histopathology studies were performed on mice aged between 2 and 6 months. After terminal exsanguination, spleens were excised and immersion-fixed overnight at 4 °C in 4% paraformaldehyde in phosphate-buffered saline (PBS), washed in PBS, then stored at 4 °C in PBS containing 0.02% sodium azide. Paraffin-embedded tissue was sectioned and stained with hematoxylin-eosin for microscopic examination.

2.4. Preparation of erythrocytes for flux studies

Blood was collected in heparinized syringes by cardiac puncture of Avertin-anesthetized mice according to protocols approved by the Institutional Animal Care and Use Committee of Beth Israel Deaconess Medical Center. Blood was centrifuged at 2500 rpm in 50 ml Falcon tubes for 5 min at 4 °C. After careful removal of the buffy coat by aspiration, packed cells were washed 5 times at 4 °C in ~20 volumes of wash solution (in mM: 172 choline Cl, 1 $MgCl_2$, 10 Tris MOPS), pH 7.40 at 4 °C. Cells were suspended to 30–50% cytocrit in wash solution and kept at 4 °C for same-day use in flux studies. Red blood cell indices were measured with the ADVIA 120™ hematology analyzer, using mouse software (Siemens Diagnostic Solutions, Tarrytown, NY) as previously described [8,19]. Total erythrocyte contents of Na^+, K^+, and Mg^{2+} were determined in freshly isolated mouse erythrocytes by atomic absorption spectrophotometry (AAnalyst 800; Perkin Elmer, Norwalk, CT) as previously described [17].

2.5. Erythrocyte Na and K fluxes

KCC activity was determined as swelling-dependent K^+ efflux in erythrocytes exposed to hypotonic swelling in the presence of 1 mM ouabain and 10 μM bumetanide as described [17–19]. Briefly, freshly isolated erythrocytes were incubated in either hypotonic or isotonic NaCl media or Na sulfamate media at pH 7.4 at 37 °C. Aliquots were removed after 5 min and 25 min incubation at 37 °C and immediately transferred to precooled 4 ml plastic tubes. Supernatant [K^+] was calculated from K content measured by atomic absorption. K^+ efflux was calculated from the slope of the linear regression of K^+ content vs time. Volume-dependent KCC activity was estimated by subtracting total Cl^--dependent K^+ efflux into hypotonic medium from that into isotonic medium. KCC activity stimulated by staurosporine or by urea was also determined from Cl^--dependent K^+ efflux measured in the absence and presence of these KCC agonists. KCC activities of red cells from WT^{Kcnn4}, WT^{SAD}, and WT^{C57} tested in isotonic and hypotonic conditions were indistinguishable (data not shown). Thus, red cells from WT mice of these distinct genetic backgrounds were combined in assays of phthalate density profile, osmotic lysis, and KCC activity.

Na/K pump and NKCC were measured as previously described [17]. Briefly, freshly isolated erythrocytes were equilibrated in 75 mM NaCl, 75 mM KCl in the presence of 40 μg/ml nystatin. Nystatin-loaded red

cells were centrifuged and washed with 0.1% bovine serum albumin fraction V (BSA) to remove nystatin, then centrifuged and washed five more times at 4 °C in choline wash solution to remove extracellular Na^+ and K^+. Washed cells suspended to ~50% cytocrit were aliquoted for the ADVIA hematology analyzer, for ion content, and for manual determination of hematocrit. The remaining nystatin-loaded cells were incubated in flux media [17], with aliquots rapidly centrifuged at appropriate times. Supernatants were carefully transferred to 4 ml plastic tubes for determination of Na and K contents by atomic absorption spectrometry. Fluxes in the presence and absence of 1 mM ouabain and/or bumetanide (1 mM or 10 μM as indicated) were calculated from linear regression slopes. Na-K pump activity was estimated as the ouabain-sensitive fraction of Na^+ efflux. NKCC activity was estimated as the 10 μM bumetanide-sensitive fraction of flux in the presence of ouabain. Na/H exchange was measured as 1 mM amiloride-sensitive flux in the presence of ouabain and bumetanide as described previously [17].

2.6. Phthalate density profile

Erythrocyte density distribution profiles of freshly obtained red cells were measured at 23 °C in microhematocrit tubes containing phthalate esters of density between 1.076 and 1.108 g/ml, as previously described [8]. The % cells of density > X was calculated from the total cell content sedimented below the phthalate oil density boundary in the lower oil zone divided by the total amount of cells. The phthalate oil D_{50} value is the 50th %ile of density of the red cell population, and describes alterations in RBC density profiles [5,6].

2.7. Osmotic fragility measurement

Osmotic fragility of erythrocytes was measured on freshly collected blood in heparin. RBCs washed 3× with choline wash solution and once in isotonic saline were resuspended at 10% cytocrit. Aliquots were suspended in varying concentrations of NaCl and centrifuged 5 min at 3000 RPM at 22 °C. The supernatant was collected and A_{540} was measured with appropriate controls to calculate values of % RBC lysis. Osmotic fragility curves were generated by plotting varying salt concentrations vs % hemolysis.

2.8. Statistical analysis

All results are expressed as means ± SEM. As the data were non-parametric, they were analyzed by ANOVA with Mann-Whitney and Kruskal-Wallis non-paired tests using Prism 8 software (GraphPad). Significance was set at $p < 0.05$.

3. Results

3.1. Hematological indices of WT and SAD mice with genetic deletion of Kcnn4, Kcc1 and Kcc3

Hematological indices of WT and SAD mice carrying genetic inactivation of *Kcnn4*, dual inactivation of *Kcc1* and *Kcc3*, and combined inactivation of all three genes are shown in Table 1. As previously described [8,18], SAD mice exhibited mild anemia characterized by reduced mean corpuscular volume (MCV), elevated corpuscular hemoglobin concentration mean (CHCM) with 2.1% hyperdense cells, elevated relative density width (RDW), and mild reticulocytosis of 3.7% vs 3.0% for WT. Genetic inactivation of *Kcnn4* produced no significant changes in hemolytic indices as compared with WT^{Kcnn4} mice. The slightly decreased CHCM and slightly increased MCV suggested a trend towards increased red cell hydration (Table 1). These are milder changes than reported previously for red cells of exon 4-deleted $Kcnn4^{-/-}$ mice [10]. However, on the SAD background *Kcnn4* inactivation slightly increased MCV and decreased CHCM without significant change in other indices. Double knockout of *Kcc1* and *Kcc3* also caused completely compensated hemolytic anemia, with macrocytosis, higher MCV and lower CHCM and RDW compared to WT^{SAD}, as described [18]. On the SAD background, deficient expression of KCC1 and KCC3 partially reversed and/or normalized these changes, most importantly, decreased the % of hyperdense cells from 2.1 to 0.4 (Table 1 and [18]).

$Kcnn4^{-/-};Kcc1^{-/-};Kcc3^{-/-}$ triple knockout mice (3xKO) [19] exhibited anemia (36 vs 42% for WT^{Kcnn4}, increased MCV (59 vs 51 fL) and decreased CHCM (26 vs 28 g/dL; Table 1), but showed no significant change in % hyperdense cells (by ANOVA considering all tested genotypes; see Table 1 legend). SAD;$Kcnn4^{-/-};Kcc1^{-/-};Kcc3^{-/-}$ (SAD;3xKO) mice exhibit lower hematocrit and higher reticulocytosis than do SAD mice, accompanied by much higher MCV (56 vs 44 fL), reduced CHCM (26 vs 32 g/dL) and greatly reduced % of hyperdense cells (0.8 vs 2.1%) (Table 1).

Thus, incremental knockout of volume regulatory transmembrane K^+ pathways leads to graded increases in MCV, from 50–51 fL (WT) to 52 ($Kcnn4^{-/-}$) to 55 (2xKO) to 59 fL (3xKO). In the SAD background MCV values increase from 44 fL to 46 (SAD;$Kcnn4^{-/-}$) to 50 (SAD;2xKO), and then to 56 fL (SAD;3xKO) (Table 1). The absence of these physiological K^+ efflux pathways antagonized and reversed red cell dehydration in SAD sickle red cells. In SAD;3xKO mice plasma LDH was lower and plasma iron higher than in SAD mice, whereas total bilirubin values were indistinguishable (Supplemental Table 1).

3.2. Splenomegaly and erythroid hyperplasia

Exon 1-deleted $Kcnn4^{-/-}$ mice exhibited splenomegaly, as previously noted for exon 4-deleted $Kcnn4^{-/-}$ mice [10], and the splenomegaly of SAD mice [24] was further increased by loss of KCNN4 (Fig. 1). No splenomegaly was evident in $Kcc1^{-/-};Kcc3^{-/-}$ (2xKO) mice on WT or SAD backgrounds, but 3xKO and SAD;3xKO mice showed the greatest splenomegaly (Fig. 1). Splenomegaly was secondary to erythroid hyperplasia and red pulp congestion with enucleate mature RBCs, with corresponding reduction in white pulp. Erythroid hyperplasia was most marked in 3xKO and SAD;3xKO spleens. Red pulp congestion was marked in SAD, and moderate in SAD;$Kcnn4^{-/-}$ and moderate in SAD;3xKO, and mild in 3xKO (Fig. 2; see also Supplemental Fig. 1 for lower magnification view). Aggregates of hemosiderin-laden macrophages were prominent in SAD and SAD;$Kcnn4^{-/-}$ mice, less prominent in $Kcnn4^{-/-}$ spleens. Thus splenomegaly and erythroid hyperplasia are associated with lack of KCNN4, but not with lack of KCC3 and/or KCC1. Erythroid hyperplasia with prominent macrophage hemosiderin was also reported in exon 4-deleted $Kcnn4^{-/-}$ mice [10].

The spleen-to-body weight ratio was sexually dimorphic in WT^{Kcnn4} mice and $Kcnn4^{-/-}$ mice, and in WT^{SAD}, SAD, SAD;$Kcnn4^{-/-}$, and SAD;3xKO mice, with relative spleen weights higher in females than males (Supplemental Table 2). This sexual dimorphism did not achieve statistical significance among WT^{C57}, 2xKO, and 3xKO mice, or among SAD;2xKO mice. Similar sexual dimorphism of mouse spleen-to-body weight ratio was previously observed in C57BL6 mice [13] and subsequently demonstrated to be regulated in part by androgen action in both females and males [14].

3.3. Red cell density, osmotic fragility, and ion content

2xKO red cells exhibited lower densities than WT cells. The less dense 70% of 3xKO red cells also exhibited reduced densities compared to WT. However, the densest 30% of 3xKO red cell did not differ in density from WT^{Kcnn4} red cells (Fig. 3A). As previously shown, RBC density is uniformly higher in SAD than WT cells (Fig. 3B, [18]). In contrast, the lightest 30–40% of $Kcnn4^{-/-}$ red cells were less dense than WT cells. SAD;$Kcnn^{4-/-}$ red cells were of much lower density than SAD red cells, with the notable exception of the densest 10% of

Table 1
Hematological indices of red cells from WT and SAD mice carrying individual and combined knockouts of *Kcnn4*, *Kcc1*, and *Kcc3*.

Genotype	Hematocrit (%)	MCV (fL)	CHCM (g/mL)	RDW (%)	Hyper (%)	Retic (%)
WT^{Kcnn4}	41.5 ± 0.5 (48)	51.3 ± 0.3 (50)	28.4 ± 0.1 (49)	13.7 ± 0.1 (48)	0.4 ± 0.1 (48)	3.0 ± 0.1 (46)
Kcnn4$^{-/-}$	41.6 ± 0.3 (58)	52.1 ± 0.4 (63)	27.5 ± 0.1 (64)	14.6 ± 0.2 (63)	0.1 ± 0.0 (63)	3.8 ± 0.1 (60)
WT^{SAD}	42.0 ± 0.3 (91)	50.1 ± 0.2 (64)	28.0 ± 0.1 (108)	13.3 ± 0.1 (110)	0.1 ± 0.0 (112)	3.0 ± 0.1 (107)
Kcc1$^{-/-}$;*Kcc3*$^{-/-}$	43.6 ± 0.2$^{\beta}$ (104)	54.8 ± 0.1$^{\beta}$ (114)	26.1 ± 0.1$^{\beta}$ (112)	12.0 ± 0.1$^{\beta}$ (115)	0.1 ± 0.0 (113)	3.0 ± 0.1 (112)
Kcnn4$^{-/-}$;*Kcc1*$^{-/-}$;*Kcc3*$^{-/-}$	35.7 ± 0.5$^{\alpha}$ (43)	59.0 ± 0.4$^{\alpha}$ (47)	26.2 ± 0.2$^{\alpha}$ (48)	14.5 ± 0.1$^{\alpha}$ (48)	0.1 ± 0.0 (47)	5.1 ± 0.3$^{\alpha}$ (48)
SAD	39.4 ± 0.4† (56)	43.8 ± 0.2† (86)	31.7 ± 0.1† (86)	18.6 ± 0.2† (84)	2.1 ± 0.2† (76)	3.7 ± 0.1† (78)
SAD;*Kcnn4*$^{-/-}$	38.2 ± 0.5 (67)	45.5 ± 0.2$^{¥}$ (87)	31.1 ± 0.1$^{¥}$ (86)	18.0 ± 0.2$^{¥}$ (86)	2.1 ± 0.3 (85)	4.0 ± 0.1 (87)
SAD;*Kcc1*$^{-/-}$;*Kcc3*$^{-/-}$	42.0 ± 0.7* (13)	50.1 ± 0.5* (14)	28.6 ± 0.3* (14)	15.0 ± 0.3* (13)	0.4 ± 0.1* (13)	3.6 ± 0.3 (13)
SAD;*Kcnn4*$^{-/-}$;*Kcc1*$^{-/-}$;*Kcc3*$^{-/-}$	32.2 ± 0.6$^{§,€}$ (30)	55.9 ± 0.4$^{§,€}$ (32)	26.2 ± 0.2$^{§,€}$ (34)	18.7 ± 0.3 (33)	0.8 ± 0.1$^{§,€}$ (34)	6.1 ± 0.3$^{§,€}$ (32)

Values are means ± SEM for (n) mice of indicated genotypes. ANOVA, Kruskal-Wallis test.
Note that the unpaired Mann-Whitney *t*-test comparing % hyperdense cells in WT^{KCNN4} and in 3xKO mice suggested significant difference ($p = 0.0003$).
$^{\alpha}$ $p < 0.001$ (WT^{SAD} vs 3xKO).
$^{\beta}$ $p < 0.05$ (WT^{SAD} vs 2xKO).
* $p < 0.05$ (SAD vs SAD;2xKO).
† $p < 0.001$ (WT^{SAD} vs SAD).
$^{€}$ $p < 0.0001$ (SAD vs SAD;3xKO).
§ $p < 0.001$ (SAD;*Kcnn4*$^{-/-}$ vs SAD;3xKO).
$^{¥}$ $p < 0.05$ (SAD vs SAD;*Kcnn4*$^{-/-}$).

SAD;*Kcnn4*$^{-/-}$ red cells, of density similar to that of the densest 10% of SAD red cells. However the less dense 80% of RBC from SAD;*Kcnn4*$^{-/-}$ and Kcnn4$^{-/-}$ mice were of significantly lower density than the corresponding fraction of SAD RBC (Fig. 3B). Genetic inactivation of KCC1 and KCC3 in SAD mice reduced red cell density of only the least dense 20% of cells compared to those of SAD mice. However, red cells of SAD;3xKO mice exhibited substantially decreased density across the entire RBC density distribution in comparison with SAD red cells (Fig. 3C). Thus genetic inactivation of *Kcnn4* or of *Kcc1;Kcc3* decreased red cell density of only the least dense RBC, but combined 3xKO leads to dramatically decreased RBC density in RBC of nearly all densities, most markedly in the SAD background.

WT red cell osmotic fragility is modestly increased by knockout of *Kcc1* and *Kcc3*, as observed previously [18], but dramatically increased by additional inactivation of *Kcnn4* in 3xKO mouse red cells (Fig. 4A). The greatly decreased osmotic fragility of SAD red cells was significantly right-shifted by either combined loss of the KCC transporters or by loss of KCNN4, but became dramatically more sensitive to osmotic lysis in the setting of genetic inactivation of all three K^+ transport pathways in SAD;3xKO mice (Fig. 4B). The osmotic fragility curve of *Kcnn4*$^{-/-}$ red cells (n = 5) was nearly indistinguishable from that of WT (not shown).

Table 2 shows contents of K, Na, and Mg as measured by atomic absorption spectrometry. As reported previously, K content of SAD red cells was lower than that of WT RBC [8]. Loss of KCNN4 alone from SAD red cells did not increase SAD red cell K content. However, combined loss of KCC1 and KCC3, or of KCNN4, KCC1 and KCC3 together restored K content of SAD red cells to levels even higher than those of WT red cells. Combined loss of KCC1 and KCC3, or of KCNN4, KCC1, and KCC3 in WT red cells also increased K content above WT level. In addition, red cells from 3xKO mice in SAD or WT backgrounds also exhibited higher Na contents than found in unmodified SAD or WT red cells. These data confirm that genetic inactivation of K^+ leak pathways increases cell K content, and can reverse red cell dehydration in the SAD model of sickle cell disease.

3.4. Ion transport activity in SAD RBC in the presence and absence of KCNN4 and KCCs

Basal KCC activity in SAD red cells was not statistically higher than that of WT cells, but hypotonicity-stimulated KCC activity in SAD red cell was elevated. In contrast, KCC activity stimulated by 1 μM staurosporine or by 500 mM urea was elevated to equivalent levels in both SAD and WT red cells (Fig. 5).

Genetic inactivation of KCNN4 in SAD red cells had no effect on either basal KCC activity or KCC stimulated by hypotonicity, staurosporine, or urea in SAD cells (Fig. 6A). In *Kcnn4*$^{-/-}$ RBC, conferral of the SAD genotype did not significantly increase basal KCC activity, or activity stimulated by staurosporine or urea, but did enhance KCC stimulation by hypotonicity (Fig. 6B). Loss of KCC activity in SAD red cells with genetically inactivated KCC1 and KCC3 was unaffected by the additional genetic absence of KCNN4 activity (Fig. 7A and data not

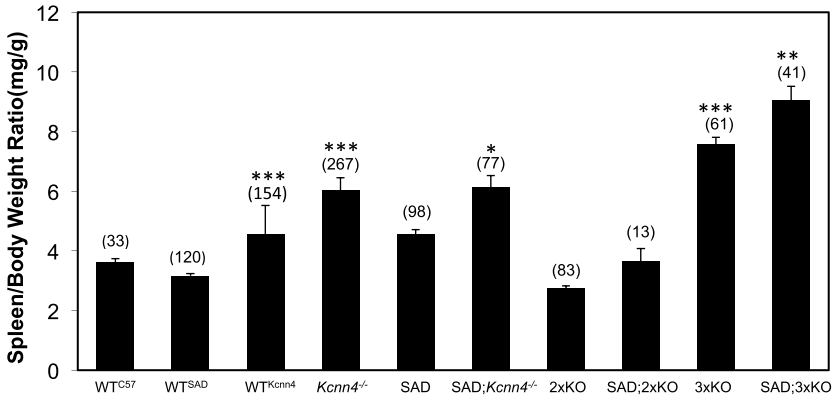

Fig. 1. Genetic deletion of *Kcnn4* increases spleen-to-body weight ratio in all tested genetic backgrounds. Values represent mean ± SEM for (n) mice of the indicated genotypes. One-way ANOVA, non-paired Kruskal-Wallis test.
*, $p < 0.02$ for comparison of SAD;*Kcnn4*$^{-/-}$ vs SAD.
**, $p < 0.003$ for comparisons of SAD;3xKO vs SAD or vs SAD;*Kcnn4*$^{-/-}$.
***, $p < 0.0001$ for comparisons of 3xKO vs WT^{Kcnn4} or vs *Kcnn4*$^{-/-}$; and for comparisons of WT^{Kcnn4} vs *Kcnn4*$^{-/-}$ or vs WT^{SAD}.

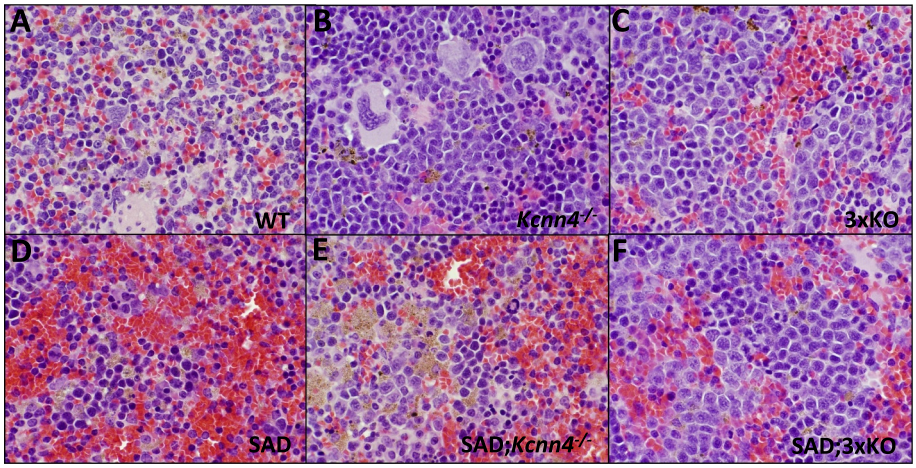

Fig. 2. Spleen histology (hematoxylin-eosin stain) of the indicated genetic backgrounds. Magnification 600×. Representative sections from the 3 mice of each indicated genotype examined.

shown), consistent with lack of significant compensatory increase in KCC4 or other K^+ uptake activity. Moreover, the very low basal KCC activity and minimal if any stimulated KCC activity in 3xKO mice was unaffected by the additional expression of the SAD sickle hemoglobin transgene (Fig. 7B). However, *Kcc1*$^{-/-}$;*Kcc3*$^{-/-}$ red cells exhibited A23187-stimulated KCNN4 activity (0.29 + 0.002 mmol/L cells × min) at 65% the stimulated KCNN4 rate in WT RBC (0.44 + 0.01 mmol/L cells × min; n = 6, not shown).

Measurements of KCC activity summarized in Figs. 5–7 were limited to experiments in which each red cell sample was tested in the presence of Cl^--containing media and SFA-containing media. Combined results from the entire study, including experiments in which red cells were tested in the presence of either Cl^-- or SFA-containing media, but not both (due to blood volume limitations or other reasons) are presented in Supplemental Fig. 2, which recapitulates the conclusions from Figs. 5–7. Red cell KCC activities of 2xKO and SAD;2xKO mice were presented previously [18].

3.5. Other red cell cation transport activities in the presence and absence of KCNN4 and KCCs

Table 3 presents the effects of selective or combined genetic inactivation of KCNN4 and/or KCCs on other red cell cation transport activities. Absence of KCNN4 function from WT red cells decreased NKCC activity to 40–45% of WT levels, whereas KCC deletion had no inhibitory effect on NKCC. However, red cells of 3xKO mice exhibited normal levels of NKCC activity. SAD red cells exhibited only ~30% of WT NKCC activity. This impaired function was unaltered by absence of KCNN4, but was partially rescued to 70% of WT levels in RBC of SAD;3xKO mice. Na^+,K^+-ATPase activity of WT red cells was affected little by genetic deletion of KCCs or of KCNN4, but was elevated by 50% in 3xKO mice. Na^+,K^+-ATPase activity in red cells of SAD;x3KO mice was also higher than that in SAD red cells. SAD red cells exhibited only 19–29% of WT Na^+/H^+ exchange activity. This reduced Na^+/H^+ exchange activity was minimally elevated by genetic inactivation of KCNN4, but was rescued to 70% of wild type activity in RBC of SAD;3xKO mice.

4. Discussion

Prevention or treatment of sickle red cell dehydration has been shown effective in reducing hemolysis in the SAD mouse model of sickle disease [8] and in human sickle disease [1,2]. However, small molecule pharmacological interventions to alleviate red cell dehydration have to date targeted only the red cell Gardos channel, KCNN4. A second major pathway controlling RBC K^+ leak is that of KCC K-Cl cotransporters, predominant among which in mouse [18] and human red cells [16] is KCC3 (with variable contributions from KCC4 and KCC1 in human red cells). Unlike KCNN4, which is selectively and potently targeted by senicapoc [1,2,9,21], and despite recent development of neuronal KCC2 inhibitors [9,20], selective and potent small molecule inhibitors of erythroid K-Cl cotransporters KCC1, KCC3, and KCC4 remain unavailable.

We chose the SAD mouse model of human SCD [24], the best mouse model of sickle red cell dehydration [8,12,18], in which to ask whether combined genetic inactivation of the major erythroid regulators of K^+ leak and volume decrease, KCNN4 and the K-Cl cotransporters KCC1 and KCC3, would ameliorate or even reverse sickle red cell dehydration in a mouse model of sickle cell disease. Previous studies have suggested that red cell KCC activity and cell dehydration can be attenuated by oral Mg^{2+} supplementation in SAD mice [7], although these findings have not been reproduced in human subjects with sickle cell disease [23]. We found that red cell dehydration of SAD mice was improved by genetic inactivation of *Kcnn4*. We further showed that combined genetic inactivation of *Kcnn4*, *Kcc1*, and *Kcc3* encoding the dominant erythroid K^+ leak pathways led to further reversal of cell dehydration, resulting in cells swollen considerably above WT volumes (Table 1). These increases in cell volume were accompanied by corresponding decreases in CHCM and cell density and by increased osmotic fragility, suggesting that combined treatment of sickle disease with the KCNN4 inhibitor senicapoc and a yet-to-be developed specific inhibitor of erythroid KCCs (or an inhibitor specifically targeting KCC3) would enhance reversal of sickle red cell dehydration to levels beyond those achieved by senicapoc treatment alone [1,2], possibly with accompanying further reductions in hemolysis. The still unexplained decrease in clinical severity of the neuronal phenotype of mouse *Kcc3* inactivation [11] by the additional inactivation of *Kcc1* (see Materials and methods) suggests the possibility that a clinically tolerable regimen of pharmacological inhibition of erythroid KCC activity might be developed without phenocopying the peripheral neurotoxicity of the *Kcc3*$^{-/-}$ mouse.

The SAD red cell volume increases produced by combined genetic inactivation of *Kcnn4*, *Kcc1*, and *Kcc3* may have reflected additional inputs beyond the loss of these corresponding K^+ transport activities. SAD;3xKO red cells revealed secondary functional increases in several transporter activities that normally mediate volume increase. These include substantial elevations in the activities of the NKCC1 $Na^+/K^+/2Cl^-$ cotransporter, the Na^+,K^+-ATPase, and the NHE1 Na^+/H^+

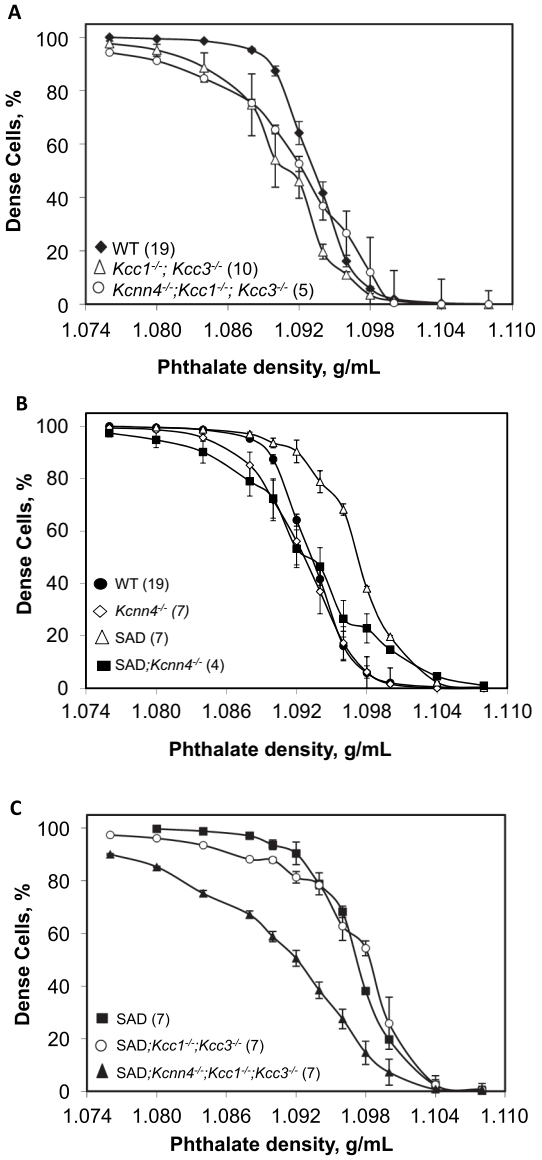

Fig. 3. Red cell phthalate density profiles as function of genotype. A. Red cells from WT mice (black diamonds) compared with red cells from *Kcc1*$^{-/-}$;*Kcc3*$^{-/-}$ mice (2xKO, open triangles) and red cells from *Kcnn4*$^{-/-}$;*Kcc1*$^{-/-}$;*Kcc3*$^{-/-}$ mice (3xKO, open circles). B. Red cells from WT (black circles, reproduced from data of panel A) and SAD mice (open triangles) compared with *Kcnn4*$^{-/-}$ mice (open diamonds) and SAD;*Kcnn4*$^{-/-}$ mice (black squares). WT mice in panels A and B included WT^{Kcnn4} (n = 8) and WT^{SAD} (n = 11), which were indistinguishable (not shown). C. Red cells from SAD mice (black squares, data replicated from panel B) compared with red cells from SAD;*Kcc1*$^{-/-}$;*Kcc3*$^{-/-}$ mice (open circles) and red cells from SAD;*Kcnn4*$^{-/-}$;*Kcc1*$^{-/-}$;*Kcc3*$^{-/-}$ mice (black triangles). Values are means ± SEM for (n) independently tested pooled samples from each indicated genotype.

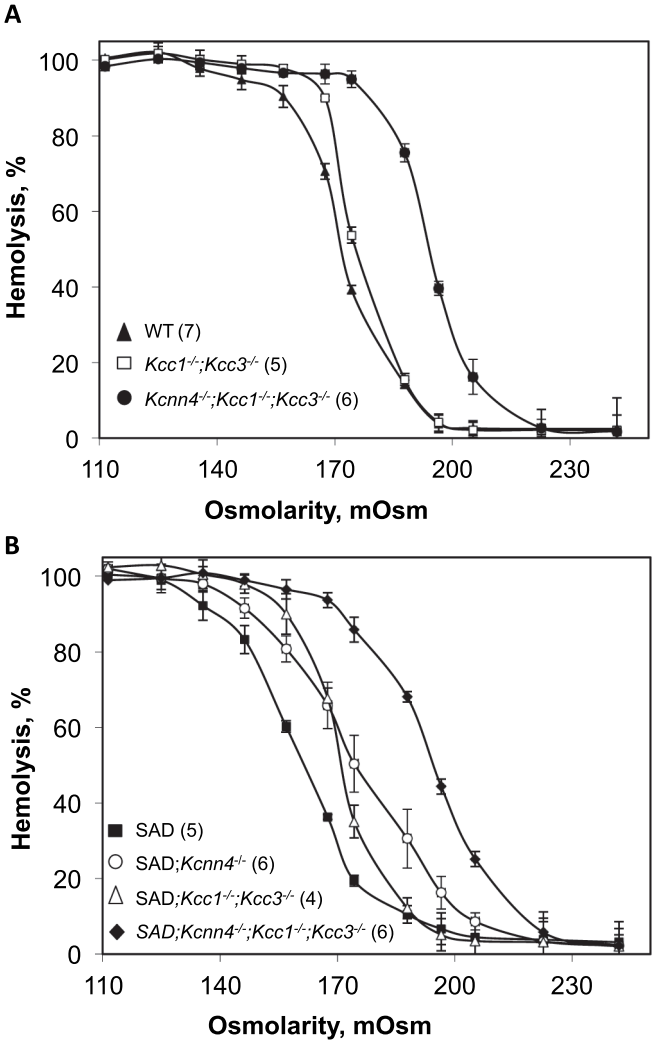

Fig. 4. Red cell susceptibility to osmotic lysis as function of genotype.
A. Osmotic lysis curves of red cells from WT mice (black triangles; pooled data from WT^{SAD} (n = 3) and WT^{Kcnn4} (n = 4)) compared with osmotic lysis curves of red cells from *Kcc1*$^{-/-}$;*Kcc3*$^{-/-}$ mice (open squares) and from *Kcnn4*$^{-/-}$;*Kcc1*$^{-/-}$;*Kcc3*$^{-/-}$ mice (black circles). B. Osmotic lysis curves SAD mice (black squares) compared with those of red cells from SAD;*Kcnn4*$^{-/-}$ mice (open circles), SAD;*Kcc1*$^{-/-}$;*Kcc3*$^{-/-}$ mice (open triangles), and SAD;*Kcnn4*$^{-/-}$;*Kcc1*$^{-/-}$;*Kcc3*$^{-/-}$ mice (black diamonds). Values are means ± SEM for (n) independently tested pooled samples from each genotype.

exchanger, all of which could contribute to the prevention and reversal of cell dehydration. The mechanisms by which these secondary changes in activities of volume-increasing transporters reinforce the loss of one or both volume decrease pathways remain unclear, but may be somehow related to the naturally wide ranges of red cell cation transport activities detected among inbred mouse strains [17].

As previously reported for the *Kcnn4*$^{-/-}$ exon 4 knockout mouse [10], the *Kcnn4*$^{-/-}$ exon 1 knockout mouse exhibited no anemia or reticulocytosis. Combined genetic inactivation of *Kccn4*, *Kcc1* and *Kcc3* mildly increased splenomegaly compared to that in *Kcnn4*$^{-/-}$ mice of either C57/Bl6 or SAD backgrounds (Fig. 1). Loss of KCNN4 was accompanied by moderate increases in reticulocytosis (Table 1) and increased plasma values of bilirubin and lactate dehydrogenase, but not iron, as compared to WT^{Kcnn4} (Supplemental Table 1). Moreover, combined genetic inactivation of *Kccn4*, *Kcc1* and *Kcc3* not only failed to improve hematocrit and reticulocytosis in SAD mice, but rather worsened these hematological indices in both WT and SAD backgrounds. Clearly, any increase in hemolytic red cell turnover in patients with sickle cell diseases would complicate their treatment. However, clinical pharmacological inhibition of red cell K transporters in patients with sickle cell disease will likely be incomplete, and thus might allow dose titration that balances potential hemolytic toxicity against therapeutic partial rehydration of pathologically dehydrated sickle red cells.

Nonetheless, we have demonstrated that combined genetic

Table 2
Cation content of red cells from WT and SAD mice carrying individual and combined knockouts of *Kcnn4*, *Kcc1* and *Kcc3*.

Genotype	[K] (mmol/kg Hb)	(n)	[Na] (mmol/kg Hb)	(n)	[Mg] (mmol/kg Hb)	(n)
WT^{Kcnn4}	429.5 ± 8.8	18	20.6 ± 0.4	19	10.0 ± 0.8	8
$Kcnn4^{-/-}$	451.1 ± 10	23	22.1 ± 0.7	22	9.4 ± 0.7	7
WT^{SAD}	419.5 ± 5.8	39	19.8 ± 0.6	40	8.2 ± 0.3	20
$Kcc1^{-/-};Kcc3^{-/-}$	457.0 ± 6.4$^{\beta}$	40	21.1 ± 0.4	39	9.6 ± 0.4	18
$Kcnn4^{-/-};Kcc1^{-/-};Kcc3^{-/-}$	468.9 ± 6.7$^{\alpha}$	22	25.7 ± 0.7$^{\alpha}$	22	9.8 ± 0.5	19
SAD	368.5 ± 8.4†	30	15.5 ± 0.5†	30	9.1 ± 0.6	17
SAD;$Kcnn4^{-/-}$	369.6 ± 6.9	29	16.7 ± 0.5	30	8.4 ± 0.3	14
SAD;$Kcc1^{-/-};Kcc3^{-/-}$	460.1 ± 57.5*	6	18.6 ± 2.1	6	9.8 ± 1.2	6
SAD;$Kcnn4^{-/-};Kcc1^{-/-};Kcc3^{-/-}$	447.6 ± 6.6$^{\epsilon}$	16	21.2 ± 0.7$^{\epsilon,\S}$	16	10.5 ± 0.4	14

Values are means ± SEM for (n) mice of indicated genotypes. ANOVA, Kruskal-Wallis test.
$^{\beta}$ $p < 0.05$ (WT^{SAD} vs 2xKO).
† $p < 0.05$ (WT^{SAD} vs SAD).
$^{\alpha}$ $p < 0.01$ (WT^{SAD} vs 3xKO).
$^{\epsilon}$ $p < 0.001$ (SAD vs SAD;3xKO).
§ $p < 0.01$ (SAD;$Kcnn4^{-/-}$ vs SAD;3xKO).
* $p < 0.05$ (SAD vs SAD;2xKO).

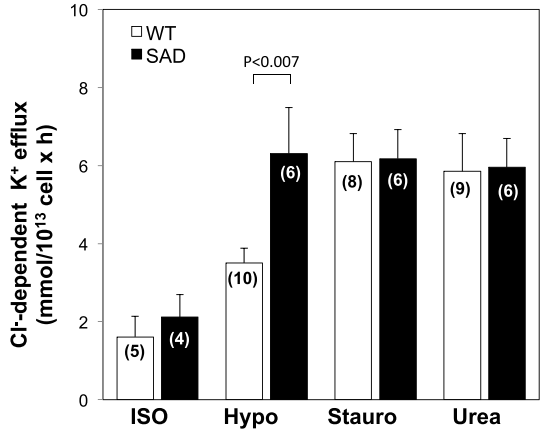

Fig. 5. Basal and stimulated K-Cl cotransport activity in WT and SAD red cells. K-Cl cotransport activity of WT and SAD red cells was measured in isotonic medium (ISO), hypotonic medium (Hypo), isotonic medium containing 1 μM staurosporine (Stauro), and isotonic medium with added 500 mM urea (Urea). Values are means ± SEM for (n) independent experiments with blood pooled from 2 to 4 mice of indicated genotype. ISO WT red cells (n = 5) included WT^{C57} (n = 2), WT^{Kcnn4} (n = 2) and WT^{SAD} (n = 1). WT red cells in stimulated conditions were (for HYPO, n = 10) 1 WT^{C57} + 9 WT^{Kcnn4}; (for Stauro, n = 8) 1 WT^{C57} + 7 WT^{Kcnn4}; and (for Urea, n = 9) 1 WT^{C57}, 1 WT^{SAD}, and 7 WT^{Kcnn4}. WT and SAD samples were compared for each condition by Mann-Whitney non-paired test.

inhibition of erythroid KCNN4 and KCC K-Cl cotransporters can rescue and even reverse the pathological red cell dehydration of sickle disease modeled in the SAD mouse. KCNN4 inhibition by senicapoc significantly reduced red cell dehydration and increased hematocrit and hemoglobin in sickle cell disease patients without promoting splenomegaly [1,2]. Should specific inhibitors of erythroid KCCs become available in the future, tests of their combined administration with senicapoc will determine whether or not they exacerbate hemolysis and anemia, and thus phenocopy the SAD;3xKO mouse.

Several strategies for gene therapy of sickle disease have recently proven successful, but their widespread adoption will be limited for the near future due to high costs and requirement for specialized medical centers. In the meantime, improved treatment of human sickle red cell dehydration combining senicapoc with a yet to be developed specific inhibitor of KCC3 (and/or KCC1 and KCC4) may ultimately prove useful as part of broader non-genetic combination therapies, including modification of HbSS oxygen binding, modification of sickle red cell adhesion to activated endothelial cells, and modification of endothelial vasodilation, among other therapeutic opportunities under investigation.

Contributions

SLA, BES and AR designed the study. CAH, MBR and MT provided genetically modified mice. BES, PB, KN, EHK, AH performed experiments and collected data. AR, BES, PB, CB, and SLA analyzed data. The manuscript was drafted by SLA, AR and BES, and reviewed by the authors.

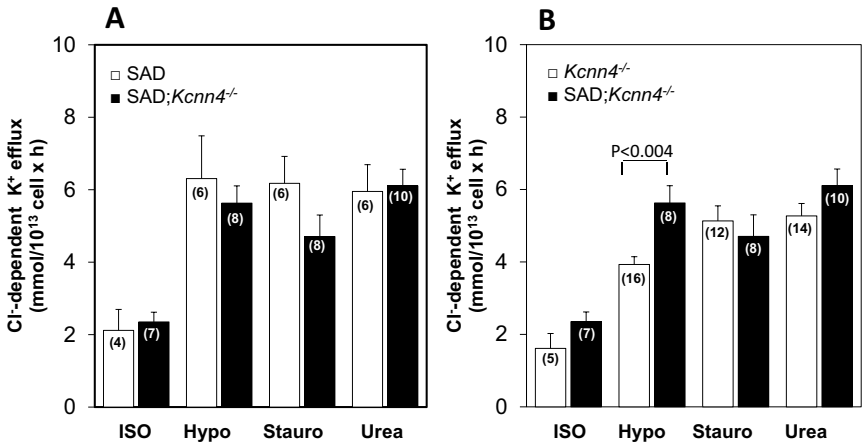

Fig. 6. Basal and stimulated K-Cl cotransport activity in SAD;$Kcnn4^{-/-}$ red cells compared with (A) SAD red cells and with (B) $Kcnn4^{-/-}$ red cells. K-Cl cotransport activity was measured in isotonic medium (ISO), hypotonic medium (Hypo), isotonic medium containing 1 μM staurosporine (Stauro), and isotonic medium with added 500 mM urea (Urea). Values are means ± SEM for (n) independent experiments with blood pooled from 2 to 4 mice of indicated genotype. WT and SAD samples were compared for each condition by Mann-Whitney non-paired test. SAD mouse data in panel A is replicated from that of Fig. 5. Data from SAD;$Kcnn4^{-/-}$ mouse red cells is replicated in panels A and B for ease of comparison.

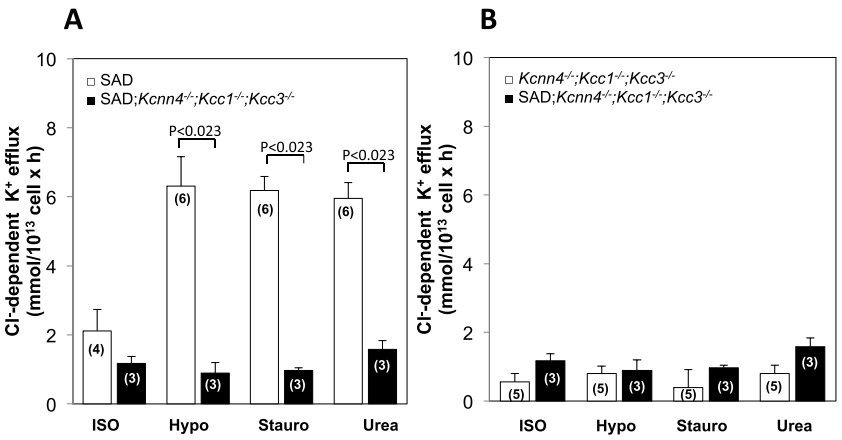

Fig. 7. Basal and stimulated K-Cl cotransport activity in red cells from SAD;*Kcnn4*$^{-/-}$;*Kcc1*$^{-/-}$;*Kcc3*$^{-/-}$ mice compared with (A) red cells from SAD mice and with (B) red cells from *Kcnn4*$^{-/-}$;*Kcc1*$^{-/-}$;*Kcc3*$^{-/-}$ mice. K-Cl cotransport activity was measured in isotonic medium (ISO), hypotonic medium (Hypo), isotonic medium containing 1 μM staurosporine (Stauro), and isotonic medium with added 500 mM urea (Urea). Values are means ± SEM for (n) independent experiments with blood pooled from 2 to 4 mice of indicated genotype. For each condition, each genotype pair was compared by Mann-Whitney non-paired test. SAD mouse data in panel A is replicated from that of Fig. 5. Data from SAD;*Kcnn4*$^{-/-}$;*Kcc1*$^{-/-}$;*Kcc3*$^{-/-}$ mouse red cells is replicated in panels A and B for ease of comparison.

Table 3
Ion transport activities of Na^+-K^+ cotransport (NKCC), Na^+,K^+-ATPase, and Na^+/H^+ exchange in red cells from WT and SAD mice carrying individual and combined knockout of *Kcnn4*, *Kcc1*, and *Kcc3*.

Genotype	n	Na^+,K^+-ATPase	$Na^+/K^+/2Cl^-$ cotransport		Na^+/H^+ exchange
		(mmol $K^+/10^{13}$ cells × h)	(mmol $K^+/10^{13}$ cells × h)	(mmol $Na^+/10^{13}$ cells × h)	(mmol $Na^+/10^{13}$ cells × h)
WT^{Kcnn4}	3	9.31 ± 3.0	8.21 ± 1.0	10.34 ± 2.0	13.3 ± 2.0
Kcnn4$^{-/-}$	3	8.93 ± 3.0	4.87 ± 0.7†	5.71 ± 0.6†	9.74 ± 2.0†
WT^{C57}	12	10.3 ± 0.7			20.3 ± 1.0
Kcc1$^{-/-}$;*Kcc3*$^{-/-}$	3	7.59 ± 3.0	7.6 ± 2.0	9.1 ± 1.0	10.3 ± 0.7
Kcnn4$^{-/-}$;*Kcc1*$^{-/-}$;*Kcc3*$^{-/-}$	4	14.2 ± 3.0$^{\beta}$	8.95 ± 0.9	12.1 ± 0.9	10.6 ± 0.8$^{\beta}$
SAD	3	15.6 ± 0.4	2.89 ± 1.0	2.8 ± 1.0	3.8 ± 0.3
SAD;*Kcnn4*$^{-/-}$	4	11.9 ± 2.0$^{\alpha}$	2.61 ± 0.7	3.19 ± 0.9$^{\alpha}$	4.68 ± 0.2$^{\alpha}$
SAD;*Kcnn4*$^{-/-}$;*Kcc1*$^{-/-}$;*Kcc3*$^{-/-}$	3	19.6 ± 0.4§	5.45 ± 0.9§	6.76 ± 1.0§	9.12 ± 0.6§

Values represent means ± SEM for (n) mice of indicated genotypes. Mann-Whitney test.
§ $p < 0.04$ (SAD vs SAD;3xKO).
$^{\alpha}$ $p < 0.04$ (SAD vs SAD;*Kcnn4*$^{-/-}$).
$^{\beta}$ $p < 0.02$ (WT^{C57} vs 3xKO).
† $p < 0.04$ (WT^{Kcnn4} vs *Kcnn4*$^{-/-}$).

Declaration of Competing Interest

The authors report no conflicts of interest related to this work.

Acknowledgements

This work was supported by NIH grant HL077765 to SLA.

Appendix A. Supplementary data

Supplementary data to this article can be found online at https://doi.org/10.1016/j.bcmd.2019.102346.

References

[1] K.I. Ataga, M. Reid, S.K. Ballas, Z. Yasin, C. Bigelow, L.S. James, W.R. Smith, F. Galacteros, A. Kutlar, J.H. Hull, J.W. Stocker, I.C.A.S. Investigators, Improvements in haemolysis and indicators of erythrocyte survival do not correlate with acute vaso-occlusive crises in patients with sickle cell disease: a phase III randomized, placebo-controlled, double-blind study of the Gardos channel blocker senicapoc (ICA-17043), Br. J. Haematol. 153 (2011) 92–104.
[2] K.I. Ataga, W.R. Smith, L.M. De Castro, P. Swerdlow, Y. Saunthararajah, O. Castro, E. Vichinsky, A. Kutlar, E.P. Orringer, G.C. Rigdon, J.W. Stocker, I.C.A. Investigators, Efficacy and safety of the Gardos channel blocker, senicapoc (ICA-17043), in patients with sickle cell anemia, Blood 111 (2008) 3991–3997.
[3] T. Begenisich, T. Nakamoto, C.E. Ovitt, K. Nehrke, C. Brugnara, S.L. Alper, J.E. Melvin, Physiological roles of the intermediate conductance, Ca2+-activated potassium channel Kcnn4, J. Biol. Chem. 279 (2004) 47681–47687.
[4] C. Brendel, S. Guda, R. Renella, D.E. Bauer, M.C. Canver, Y.J. Kim, M.M. Heeney, D. Klatt, J. Fogel, M.D. Milsom, S.H. Orkin, R.I. Gregory, D.A. Williams, Lineage-specific BCL11A knockdown circumvents toxicities and reverses sickle phenotype, J. Clin. Invest. 126 (2016) 3868–3878.
[5] C. Brugnara, L. De Franceschi, S.L. Alper, Ca(2+)-activated K+ transport in erythrocytes. Comparison of binding and transport inhibition by scorpion toxins, J. Biol. Chem. 268 (1993) 8760–8768.
[6] D. Danon, V. Marikovsky, Determination of density distribution of red cell population, J. Lab. Clin. Med. 64 (1964) 668–674.
[7] L. De Franceschi, Y. Beuzard, H. Jouault, C. Brugnara, Modulation of erythrocyte potassium chloride cotransport, potassium content, and density by dietary magnesium intake in transgenic SAD mouse, Blood 88 (1996) 2738–2744.
[8] L. De Franceschi, N. Saadane, M. Trudel, S.L. Alper, C. Brugnara, Y. Beuzard, Treatment with oral clotrimazole blocks Ca(2+)-activated K+ transport and reverses erythrocyte dehydration in transgenic SAD mice. A model for therapy of sickle cell disease, J. Clin. Invest. 93 (1994) 1670–1676.
[9] E. Delpire, A. Baranczak, A.G. Waterson, K. Kim, N. Kett, R.D. Morrison, J.S. Daniels, C.D. Weaver, C.W. Lindsley, Further optimization of the K-Cl cotransporter KCC2 antagonist ML077: development of a highly selective and more potent in vitro probe, Bioorg. Med. Chem. Lett. 22 (2012) 4532–4535.
[10] I. Grgic, B.P. Kaistha, S. Paschen, A. Kaistha, C. Busch, H. Si, K. Kohler, H.P. Elsasser, J. Hoyer, R. Kohler, Disruption of the Gardos channel (KCa3.1) in mice causes subtle erythrocyte macrocytosis and progressive splenomegaly, Pflugers Arch. 458 (2009) 291–302.
[11] H.C. Howard, D.B. Mount, D. Rochefort, N. Byun, N. Dupre, J. Lu, X. Fan, L. Song, J.B. Riviere, C. Prevost, J. Horst, A. Simonati, B. Lemcke, R. Welch, R. England, F.Q. Zhan, A. Mercado, W.B. Siesser, A.L. George Jr., M.P. McDonald, J.P. Bouchard, J. Mathieu, E. Delpire, G.A. Rouleau, The K-Cl cotransporter KCC3 is mutant in a severe peripheral neuropathy associated with agenesis of the corpus callosum, Nat. Genet. 32 (2002) 384–392.
[12] Y. Ilboudo, P. Bartolucci, A. Rivera, J.C. Sedzro, M. Beaudoin, M. Trudel, S.L. Alper, C. Brugnara, F. Galacteros, G. Lettre, Genome-wide association study of erythrocyte density in sickle cell disease patients, Blood Cells Mol. Dis. 65 (2017) 60–65.
[13] E.H. Kajioka, M.L. Andres, G.A. Nelson, D.S. Gridley, Immunologic variables in male and female C57BL/6 mice from two sources, Comp. Med. 50 (2000) 288–291.
[14] H.E. MacLean, A.J. Moore, S.A. Sastra, H.A. Morris, A. Ghasem-Zadeh, K. Rana, A.M. Axell, A.J. Notini, D.J. Handelsman, E. Seeman, J.D. Zajac, R.A. Davey, DNA-binding-dependent androgen receptor signaling contributes to gender differences and has physiological actions in males and females, J. Endocrinol. 206 (2010) 93–103.
[15] S.H. Orkin, D.E. Bauer, Emerging genetic therapy for sickle cell disease, Annu. Rev. Med. 70 (2019) 257–271.

[16] D. Pan, T.A. Kalfa, D. Wang, M. Risinger, S. Crable, A. Ottlinger, S. Chandra, D.B. Mount, C.A. Hubner, R.S. Franco, C.H. Joiner, K-Cl cotransporter gene expression during human and murine erythroid differentiation, J. Biol. Chem. 286 (2011) 30492–30503.
[17] A. Rivera, R.Y. Zee, S.L. Alper, L.L. Peters, C. Brugnara, Strain-specific variations in cation content and transport in mouse erythrocytes, Physiol. Genomics 45 (2013) 343–350.
[18] M.B. Rust, S.L. Alper, Y. Rudhard, B.E. Shmukler, R. Vicente, C. Brugnara, M. Trudel, T.J. Jentsch, C.A. Hubner, Disruption of erythroid K-Cl cotransporters alters erythrocyte volume and partially rescues erythrocyte dehydration in SAD mice, J. Clin. Invest. 117 (2007) 1708–1717.
[19] B.E. Shmukler, A. Hsu, J. Alves, M. Trudel, M.B. Rust, C.A. Hubner, A. Rivera, S.L. Alper, N-ethylmaleimide activates a Cl(−)-independent component of K(+) flux in mouse erythrocytes, Blood Cells Mol. Dis. 51 (2013) 9–16.
[20] I. Spoljaric, A. Spoljaric, M. Mavrovic, P. Seja, M. Puskarjov, K. Kaila, KCC2-mediated Cl(−) extrusion modulates spontaneous hippocampal network events in perinatal rats and mice, Cell Rep. 26 e1073 (2019) 1073–1081.
[21] J.W. Stocker, L. De Franceschi, G.A. McNaughton-Smith, R. Corrocher, Y. Beuzard, C. Brugnara, ICA-17043, a novel Gardos channel blocker, prevents sickled red blood cell dehydration in vitro and in vivo in SAD mice, Blood 101 (2003) 2412–2418.
[22] M.J. Telen, P. Malik, G.M. Vercellotti, Therapeutic strategies for sickle cell disease: towards a multi-agent approach, Nat. Rev. Drug Discov. 18 (2019) 139–158.
[23] N.N. Than, H.H.K. Soe, S.K. Palaniappan, A.B. Abas, L. De Franceschi, Magnesium for treating sickle cell disease, The Cochrane Database of Systematic Reviews, vol. 4, 2017CD011358.
[24] M. Trudel, N. Saadane, M.C. Garel, J. Bardakdjian-Michau, Y. Blouquit, J.L. Guerquin-Kern, P. Rouyer-Fessard, D. Vidaud, A. Pachnis, P.H. Romeo, et al., Towards a transgenic mouse model of sickle cell disease: hemoglobin SAD, EMBO J. 10 (1991) 3157–3165.
[25] R.E. Ware, M. de Montalembert, L. Tshilolo, M.R. Abboud, Sickle cell disease, Lancet (2017).
[26] R.E. Ware, J.M. Despotovic, N.A. Mortier, J.M. Flanagan, J. He, M.P. Smeltzer, A.C. Kimble, B. Aygun, S. Wu, T. Howard, A. Sparreboom, Pharmacokinetics, pharmacodynamics, and pharmacogenetics of hydroxyurea treatment for children with sickle cell anemia, Blood 118 (2011) 4985–4991.